IEEE Access
Multidisciplinary | Rapid Review | Open Access Journal

SPECIAL SECTION ON MISSION CRITICAL SENSORS AND SENSOR NETWORKS (MC-SSN)

Received July 9, 2019, accepted July 15, 2019, date of publication July 18, 2019, date of current version August 14, 2019.

Digital Object Identifier 10.1109/ACCESS.2019.2929870

Localization of Unmanned Aerial Vehicle Operators Based on Reconnaissance Plane With Multiple Array Sensors

JIAQI ZHEN, (Member, IEEE)
College of Electronic Engineering, Heilongjiang University, Harbin 150080, China
e-mail: zhenjiaqi2011@163.com

This work was supported in part by the National Natural Science Foundation of China under Grant 61501176, in part by the Natural Science Foundation of Heilongjiang Province under Grant F2018025, and in part by the Postdoctoral Scientific Research Developmental Fund of Heilongjiang Province under Grant LBH-Q17149.

ABSTRACT For the sake of positioning the illegal unmanned aerial vehicle operators, the paper proposes a direction of arrival (DOA) estimation algorithm based on the reconnaissance plane with multiple array sensors. First, the number of unmanned aerial vehicle signals is determined by information theory criteria. Then combined support vector regression, the direction of the operator is calculated according to some approximating function through training. Finally, the location can be estimated by integrating the DOAs acquired with the array sensors on the reconnaissance aircraft. This algorithm is convenient and fast to be realized, moreover, as a result of adopting super resolution and multiple kernel learning, it can locate numerous radio signals simultaneously and performs well in the circumstance that signals impinge on the sensor array with small-angle interval, as well as the conditions of small samples and low signal to noise ratio, besides, the algorithm also applies to the array which gain-phase inconsistency exists among the sensors.

INDEX TERMS Sensor array, radio positioning, direction of arrival, support vector regression, gain-phase inconsistency.

I. INTRODUCTION

In recent years, industry of civil unmanned aerial vehicle (UAV) has risen rapidly and shown a blowout growth [1]–[4], it is widely used in aerial photography, survey, rescue, mapping, and other civil fields. At the same time, due to the simple structure, good maneuverability, and low cost, it also applies in military surveillance and reconnaissance. Compared with other tools, UAV has many unique superiorities, for example, because of its flexibility in three-dimensional space, it can work in harsh terrain environments, such as massif, forest, buildings, and carry some hardware modules. However, the illegal flights without permission often happen. UAV is small, strong concealment, easy to be acquired and manipulated, so government, military areas, important enterprises, and some major events are likely to be invaded. In order to guard against these intruders, on one hand, they should be managed and controlled strictly, on the other hand, it is seen in Fig.1, we can locate these operators directly through finding corresponding radio signals.

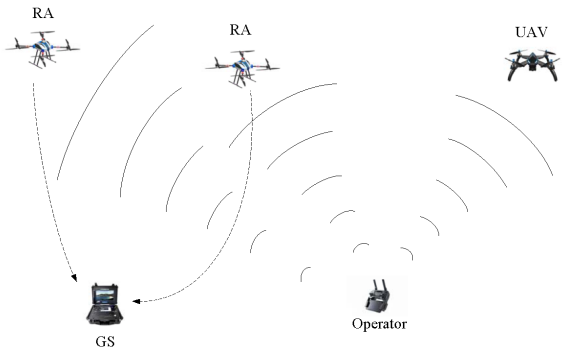

FIGURE 1. Locate the operator of the UAV.

The common information available of range-based localization algorithms includes direction of arrival (DOA) [5]–[8], time of arrival (TOA) [9]–[11], time difference of arrival (TDOA) [12]–[14], angle of arrival (AOA) [15]–[17], and received signal strength indication (RSSI) [18]–[22]. For the

The associate editor coordinating the review of this manuscript and approving it for publication was Qilian Liang.

sake of improving the location precision, Shalaby *et al.* [23] proposed a TOA algorithm with virtual anchor node and linear least square method, and it is not easily affected by noise. Tomic *et al.* [24] transformed positioning question into generalized trust region sub-problem, whose computation complexity is linear relation with the number of reference nodes. Pak *et al.* [25] employed multiple distributed and mixed particle finite impulse response filters to recognize the abnormal measure caused by non-line of sight. Liu *et al.* [26] used two-stage weighted least squares to estimate TDOA, and a better robustness was acquired. Shao *et al.* [27] utilized auxiliary variables to construct a linear least squares self-positioning problem, then decreased the error by bias compensates for pseudo-linear estimation, the local minima and divergence in iterative estimation was averted. As RSSI is vulnerable to multipath fading, noise, and other environmental parameters, Gui *et al.* [28] exploited a multiplication distance correction factor to counteract estimation error, improved the accuracy significantly. Based on spear framework, Angjelichinoski *et al.* [29] proposed a reliable solution for locating non-Bayesian sources, obtained the source, and uncertain anchor node positions simultaneously. Gustafsson and Gunna [30] used the difference between the estimated and the actual distance of the unknown and its surrounding anchor nodes to proposed a weighted centroid localization algorithm, it was also verified by ZigBee experiment. Singh and Khilar [31] designed a range-free location algorithm based on moving anchor node, but the progressive updating location of anchor node itself was ignored.

In various methods of locating targets by using their own radiation signals, DOA estimation is one of the most direct and convenient method, it is the foundation of all positioning technology, meanwhile, less equipments and amount of calculation are required, it has a high application prospect and research value. Moreover, in nowadays complex wireless environment, the direction information has become one of the most credible parameter. The classic DOA algorithms include multiple signal classification (MUSIC) [32], estimation of signal parameters via rotational invariance techniques [33] and maximum likelihood [34] algorithm, they all have a large amount of computation, bad realtime performance and cannot adapt to the real practical environment. So recently, some intelligent DOA estimation algorithms, such as machine learning and soft modeling have been concerned by the scholars at home and abroad, their main advantage is that nonlinear modeling is implemented through training samples instead of exact equation, thus, the actual noise, signal model, sensor characteristic can also be considered, meanwhile, eigen-decomposition and peak searching are avoided. Gonnouni *et al.* [35] combined support vector machine (SVM) and MUSIC to find the direction of coherent signals. Dehghanpour *et al.* [36] used multiple kernel learning (MKL) and SVM to cope with mutual coupling among sensors in DOA estimation. Gao *et al.* [37] employed sparse recovery and SVM to deal with DOA estimation in massive MIMO systems. Wang *et al.* [38] designed SVM based on deep neural network, acquiring good generalization and classification performance.

This paper proposes an algorithm for determining the position of UAV operator, based on support vector regression (SVR), reconnaissance aircraft (RA) is employed to estimate the DOA, then the result is transmitted to the ground station (GS) for the location of the operator according to their geometrical relationship, moreover, due to the use of super-resolution algorithm, we can monitor multiple UAV operators simultaneously, and the algorithm also applies to the circumstance of gain-phase errors exist among the sensors.

II. SIGNAL MODEL

The two-point positioning model is shown in Fig.2, there are B UAVs flying in the sky and respectively controlled by B operators on the ground. The positioning system is composed of one GS and two RAs, for the sake of mathematical derivation, we define the former locates at the origin, and RA1 with coordinate $(0, 0, z_1)$ flies on top of GS, RA2 $(x_2, 0, z_2)$ is in XOZ flat, the radio signal sending by the operator is used for the positioning.

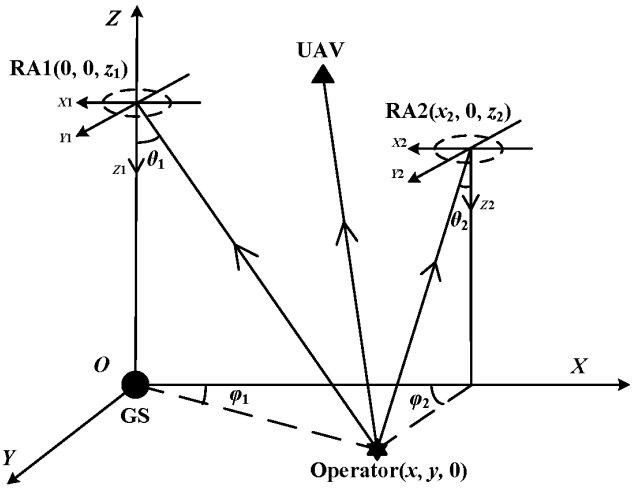

FIGURE 2. Two-point positioning model.

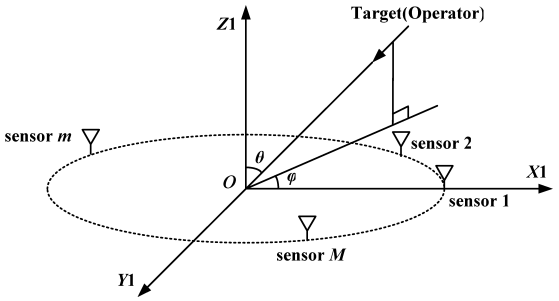

FIGURE 3. Array model of RA1.

As is shown in Fig.3, the two RAs are separately composed of airscrews, motor, and uniform circle array (UCA) with M sensors, there are B operator signals arriving at the array sensors on RAs, the center of every RA is defined as its origin,

radius is r, φ and θ are respectively the azimuth and elevation. In fact, the proposed algorithm is also suitable for the planar arrays in any forms, but the circular array is very suitable for the structural installation of reconnaissance aircraft.

A. SIGNAL MODEL UNDER IDEAL ARRAY

Take RA1 for example, under ideal array, we can acquire the array data from the targets

$$\begin{aligned}\boldsymbol{P}(t) &= \begin{bmatrix} p_1(t) \\ \vdots \\ p_m(t) \\ \vdots \\ p_M(t) \end{bmatrix} \\ &= \begin{bmatrix} \sum_{b=1}^{B} s_b(t-\tau_{1b}) \\ \vdots \\ \sum_{b=1}^{B} s_b(t-\tau_{mb}) \\ \vdots \\ \sum_{b=1}^{B} s_b(t-\tau_{Mb}) \end{bmatrix} + \begin{bmatrix} n_1(t) \\ \vdots \\ n_m(t) \\ \vdots \\ n_M(t) \end{bmatrix} \\ &= \boldsymbol{A}(\varphi,\theta)\boldsymbol{S}(t) + \boldsymbol{N}(t). \end{aligned} \tag{1}$$

where $s_b(t)$ is the bth signal, $\tau_{mb} = \frac{r}{c}\cos(\frac{2\pi(m-1)}{M} - \varphi_b)\cos\theta_b$ is the delay for the bth source arriving at the mth sensor versus origin, $p_m(t)$ is the received data of the mth sensor, $n_m(t)$ is the corresponding noise obeying Gaussian distribution, c is the signal velocity, and array manifold is

$$\begin{aligned}\boldsymbol{A}(\varphi,\theta) &= [\boldsymbol{a}(\varphi_1,\theta_1)\cdots\boldsymbol{a}(\varphi_B,\theta_B)] \\ &= \begin{bmatrix} \mathrm{e}^{-\mathrm{j}2\pi f\tau_{11}} & \cdots & \mathrm{e}^{-\mathrm{j}2\pi f\tau_{1B}} \\ \vdots & & \\ \mathrm{e}^{-\mathrm{j}2\pi f\tau_{m1}} & \cdots & \mathrm{e}^{-\mathrm{j}2\pi f\tau_{mB}} \\ \vdots & & \\ \mathrm{e}^{-\mathrm{j}2\pi f\tau_{M1}} & \cdots & \mathrm{e}^{-\mathrm{j}2\pi f\tau_{MB}} \end{bmatrix}. \end{aligned} \tag{2}$$

suppose that sampling times is T, the covariance of received data is

$$\boldsymbol{R} = \frac{1}{T}\boldsymbol{P}\boldsymbol{P}^{\mathrm{H}} = \boldsymbol{A}(\varphi,\theta)\boldsymbol{R}_{\mathrm{S}}\boldsymbol{A}^{\mathrm{H}}(\varphi,\theta) + \boldsymbol{R}_{\mathrm{N}}. \tag{3}$$

here, $()^{\mathrm{H}}$ means solving conjugate transpose, then eigen-decomposition is performed, we have

$$\boldsymbol{R} = \boldsymbol{U}\boldsymbol{\Sigma}\boldsymbol{U}^{\mathrm{H}} = \boldsymbol{U}_{\mathrm{S}}\boldsymbol{\Sigma}_{\mathrm{S}}{\boldsymbol{U}_{\mathrm{S}}}^{\mathrm{H}} + \boldsymbol{U}_{\mathrm{N}}\boldsymbol{\Sigma}_{\mathrm{N}}{\boldsymbol{U}_{\mathrm{N}}}^{\mathrm{H}}. \tag{4}$$

where

$$\boldsymbol{\Sigma} = \begin{bmatrix} \lambda_1 & & & \\ & \lambda_2 & & \\ & & \ddots & \\ & & & \lambda_M \end{bmatrix}. \tag{5}$$

is the eigenvalue matrix, $\boldsymbol{U}_{\mathrm{S}}$ and $\boldsymbol{U}_{\mathrm{N}}$ are separately the signal and noise subspace. Based on $\boldsymbol{\Sigma}$, we can use some criterion [39], [40] to detect signal number first, then determine the relevance between DOA and eigenvector $\boldsymbol{U}$. In fact, $\boldsymbol{U}_{\mathrm{S}}$ includes the signal information, and it is simpler than $\boldsymbol{U}$, and $\boldsymbol{U}_{\mathrm{N}}$ does not includes any useful information, so we can find the relationship between $\boldsymbol{U}_{\mathrm{S}}$ and DOA instead: $(\varphi,\theta)\rightarrow F(\boldsymbol{U}_{\mathrm{S}})$, then DOA estimation can be deemed to be the approximation of nonlinear function $F(\boldsymbol{U}_{\mathrm{S}})$ which can be acquired by learning.

B. SIGNAL MODEL UNDER ARRAY WITH GAIN-PHASE INCONSISTENCY

Most classic direction finding algorithms are based on the ideal array sensors, but the practical circumstance is more complicated: the inconsistent amplifiers and length among the sensors will separately cause gain and phase errors, define the first sensor as the reference, then the received data at the moment can be written in another form

$$\begin{aligned}\boldsymbol{P}'(t) &= \begin{bmatrix} p'_1(t) \\ \vdots \\ p'_m(t) \\ \vdots \\ p'_M(t) \end{bmatrix} \\ &= \boldsymbol{A}'(\varphi,\theta)\boldsymbol{S}(t) + \boldsymbol{N}(t) \\ &= \boldsymbol{W}\boldsymbol{A}(\varphi,\theta)\boldsymbol{S}(t) + \boldsymbol{N}(t). \end{aligned} \tag{6}$$

where

$$\boldsymbol{A}'(\varphi,\theta) = [\boldsymbol{a}'(\varphi_1,\theta_1)\cdots\boldsymbol{a}'(\varphi_B,\theta_B)]. \tag{7}$$

is the array manifold with gain-phase inconsistency, and

$$\boldsymbol{W} = \mathrm{diag}([1, W_2, \cdots, W_m, \cdots, W_M]^{\mathrm{T}}). \tag{8}$$

where $\mathrm{diag}(\boldsymbol{A})$ denotes diagonal matrix composed by vector $\boldsymbol{A}$, $[\boldsymbol{B}]^{\mathrm{T}}$ represents solving transposition of $\boldsymbol{B}$, and

$$W_m = \rho_m\exp(\mathrm{j}\phi_m), \quad (m = 1, 2, \cdots, M). \tag{9}$$

here, ρ_m, ϕ_m are respectively the gain and phase of the mth sensor versus the reference, then the steering vector at present is

$$\begin{aligned}\boldsymbol{a}'(\varphi_b,\theta_b) &= \mathrm{diag}([1,\cdots,W_m,\cdots,W_M]^{\mathrm{T}})\boldsymbol{a}(\varphi_b,\theta_b) \\ &= \boldsymbol{W}\boldsymbol{a}(\varphi_b,\theta_b). \end{aligned} \tag{10}$$

then we can also acquire the relation between the eigen-vector and DOA at the moment $(\varphi,\theta)\rightarrow F(\boldsymbol{U'}_{\mathrm{S}})$.

III. SUPPORT VECTOR REGRESSION

A. TRADITIONAL SUPPORT VECTOR REGRESSION

The purpose of SVR is to find a following line which approximates all the points, so that the future data can be forecasted.

$$F(\boldsymbol{x}) = \boldsymbol{w}^{\mathrm{T}}\boldsymbol{x} + b. \tag{11}$$

It has been applied in recognition of face, character, behavior, and gesture. Given a set of samples $D = [(x_1, y_1), (x_2, y_2), \cdots (x_m, y_m)]$, we want to learn a regression model

which makes $F(\boldsymbol{x})$ to be as close as possible to y, while we can tolerate at most ϵ deviations between $F(\boldsymbol{x})$ and y, then the problem is written

$$\min_{\boldsymbol{w},b} \frac{1}{2}\|\boldsymbol{w}\|^2 + C\sum_{i=1}^{m} l_\epsilon(F(x_i) - y_i). \tag{12}$$

where C is the regularization constant, l_ϵ is the ϵ-insensitive loss function

$$l_\epsilon(z) = \begin{cases} 0, & \text{if } |z| \le \epsilon; \\ |z| - \epsilon, & \text{otherwise.} \end{cases} \tag{13}$$

introduce the slack variable ξ_i and $\hat{\xi}_i$, equation (12) is rewritten as

$$\begin{aligned} \min_{\boldsymbol{w},b,\xi_i,\hat{\xi}_i} & \frac{1}{2}\|\boldsymbol{w}\|^2 + C\sum_{i=1}^{m} l_\epsilon(\xi_i + \hat{\xi}_i) \\ \text{s.t. } & F(x_i) - y_i \le \epsilon + \xi_i \\ & y_i - F(x_i) \le \epsilon + \hat{\xi}_i \\ & \xi_i \ge 0, \hat{\xi}_i \ge 0, \quad i = 1, 2, \cdots m. \end{aligned} \tag{14}$$

then introduce lagrangian multiplier $\mu_i \ge 0, \hat{\mu}_i \ge 0, \alpha \ge 0, \hat{\alpha} \ge 0$, lagrangian function of (14) can be obtained

$$\begin{aligned} L = & \frac{1}{2}\|\boldsymbol{w}\|^2 + C\sum_{i=1}^{m}(\xi_i + \hat{\xi}_i) - \sum_{i=1}^{m}\mu_i\xi_i - \sum_{i=1}^{m}\hat{\mu}_i\hat{\xi}_i \\ & + \sum_{i=1}^{m}\alpha_i(F(x_i) - y_i - \epsilon - \xi_i) \\ & + \sum_{i=1}^{m}\hat{\alpha}_i(y_i - F(x_i) - \epsilon - \hat{\xi}_i). \end{aligned} \tag{15}$$

take (11) into (15), then set the partial derivative of L to $\boldsymbol{w}$, b, ξ_i, and $\hat{\xi}_i$ equal zero respectively, then

$$\boldsymbol{w} = \sum_{i=1}^{m}(\hat{\alpha}_i - \alpha_i)\boldsymbol{x}_i. \tag{16}$$

$$0 = \sum_{i=1}^{m}(\hat{\alpha}_i - \alpha_i). \tag{17}$$

$$C = \alpha_i + \mu_i. \tag{18}$$

$$C = \hat{\alpha}_i + \hat{\mu}_i. \tag{19}$$

bring (16)-(19) into (15), we can get the dual problem of SVR

$$\begin{aligned} \max_{\boldsymbol{\alpha},\hat{\boldsymbol{\alpha}}} & \sum_{i=1}^{m} y_i(\hat{\alpha}_i - \alpha_i) - \epsilon(\hat{\alpha}_i + \alpha_i) \\ & - \frac{1}{2}\sum_{i=1}^{m}\sum_{j=1}^{m}(\hat{\alpha}_i - \alpha_i)(\hat{\alpha}_j - \alpha_j)\boldsymbol{x}_i{}^{\mathrm{T}}\boldsymbol{x}_j \\ \text{s.t. } & \sum_{i=1}^{m}(\hat{\alpha}_i - \alpha_i) = 0, \\ & 0 \le \alpha_i, \quad \hat{\alpha}_i \le C. \end{aligned} \tag{20}$$

then regression function can be written

$$F(\boldsymbol{x}) = \sum_{i=1}^{l}(-a_i + a_i^*)\kappa(\boldsymbol{x}, \boldsymbol{x}_i) + b. \tag{21}$$

Theoretically, the traditional Gaussian kernel can approximate any nonlinear one, so we choose it to construct SVR, that is

$$\kappa(\boldsymbol{x}, \boldsymbol{x}_i) = \exp\Big(-\frac{\|\boldsymbol{x} - \boldsymbol{x}_i\|^2}{2\sigma^2}\Big). \tag{22}$$

B. MULTIPLE KERNEL LEARNING

MKL is a kind of more flexible learning method and another important research direction at present. It has been verified by lots of theories and applications that traditional learning method based on single kernel model cannot handle all the samples well when the sample size is large, the sample includes heterogeneous information, sample data are irregular, or they are unevenly distributed in feature space, so fusing multiple uncertain kernels reasonably is the inevitable choice to get better learning performance at these complex circumstances.

Generally speaking, MKL integrates multiple kernel functions to acquire better performance, the kernel function can be different forms or parameters, the rich combinations enhance the expression probability greatly. Actually, the presentation of samples in high feature space is the selection of the basis kernel function and combination coefficients, different kernel functions have their unique mapping characteristics, combining these kernel functions is equivalent to join multiple high dimensional feature mapping space, thus heterogeneous samples can make full use of advantages of multiple feature spaces to represent the data better in new high dimensional feature space. Finally, the classification performance of the learning is greatly improved, hence, how to obtain a proper combination in high dimensional feature space, namely learning a suitable groups of kernel combination coefficients is the essence of MKL.

For these multiple kernel functions, the basic method is to put them together in convex combinations below

$$\kappa(\boldsymbol{x}, \boldsymbol{x}_i) = \sum_{g=1}^{G} q_g\kappa_g(\boldsymbol{x}, \boldsymbol{x}_i) \ \text{ s.t. } \ q_g \ge 0, \sum_{g=1}^{G} q_g = 1. \tag{23}$$

where G is the total number of kernels, q_g is the corresponding combination coefficient, $\kappa_g(\boldsymbol{x}, \boldsymbol{x}_i)$ is the gth classic kernel function, they can be different forms, or have disparate parameters. In our proposed algorithm, the main task of MKL is to determine the relevant coefficients a_i and q_g.

IV. DOA ESTIMATION BASED ON SVR

The idea of SVR is based on Mercer core expansion, we can map the sample data into a higher dimensional space, then define optimal linear regression super plane, thus searching for the plane comes down to convex optimization in condition of some constraints [41], [42], we construct the regression function of DOA estimation in high-dimensional space

$$F(\boldsymbol{U}_{\mathrm{S}}) = \sum_{i=1}^{l}(-a_i + a_i^*)\kappa(\boldsymbol{U}_{\mathrm{S}i}, \boldsymbol{U}_{\mathrm{S}}) + b. \tag{24}$$

where l is the number of support vectors, $\boldsymbol{U}_{Si}$ is the sample factor vector, $\boldsymbol{U}_S$ is the input eigenvector, a_i and b are the coefficients to be determined in SVR, where σ is the kernel parameter, so we can get the mapping relation based on traditional single kernel with Gaussian kernel function

$$(\varphi, \theta) \rightarrow \sum_{i=1}^{l} (-a_i + a_i^*) \exp\Big(- \frac{\|\boldsymbol{x} - \boldsymbol{x}_i\|^2}{2\sigma^2} \Big) + b. \quad (25)$$

meanwhile, we can also evaluate DOA by MKL below

$$(\varphi, \theta) \rightarrow \sum_{i=1}^{l} \sum_{g=1}^{G} (-a_i + a_i^*) q_g \kappa_g(\boldsymbol{x}, \boldsymbol{x}_i) + b. \quad (26)$$

we know from (8), DOA can be approximated by determining these unknown parameters through training, and the computation complexity of SVR mainly depends on number of support vectors, not training sample number or dimension of eigen-space, as a result of support vector selection and non-linear mapping of kernel function, the accuracy of the prediction has not decreased.

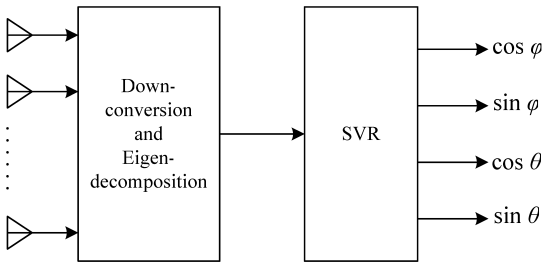

FIGURE 4. SVR Model.

In the course of modeling the DOA, its discontinuity will cause approximation error. In order to insure the continuity of output function, we use trigonometric to transform the net output into continuous value, then approximate the function. It is seen from Fig.4, the signal is received by the array sensors, then down-conversion and eigen-decomposition are successively performed to give SVR the characteristic, after that we employ SVR to approximate the DOA. In SVR model, there are four output nodes: cosφ, sinφ, cosθ, sinθ, then the DOA is

$$\begin{cases} \varphi = \arctan\Big(\dfrac{\sin\varphi}{\cos\varphi}\Big), \quad \theta = \arctan\Big(\dfrac{\sin\theta}{\cos\theta}\Big), \\ \quad \text{if } \varphi \in (0, \pi/2) \\ \varphi = \pi + \arctan\Big(\dfrac{\sin\varphi}{\cos\varphi}\Big), \quad \theta = \arctan\Big(\dfrac{\sin\theta}{\cos\theta}\Big), \\ \quad \text{if } \varphi \in (\pi/2, \pi) \\ \varphi = \pi + \arctan\Big(\dfrac{\sin\varphi}{\cos\varphi}\Big), \quad \theta = \arctan\Big(\dfrac{\sin\theta}{\cos\theta}\Big), \\ \quad \text{if } \varphi \in (\pi, \dfrac{3}{2}\pi) \\ \varphi = 2\pi + \arctan\Big(\dfrac{\sin\varphi}{\cos\varphi}\Big), \quad \theta = \arctan\Big(\dfrac{\sin\theta}{\cos\theta}\Big), \\ \quad \text{if } \varphi \in (\dfrac{3}{2}\pi, 2\pi) \end{cases} \quad (27)$$

Define the position coordinates of the operator as $(x, y, 0)$, the following equation can be established according to the geometrical relationship in Fig.2

$$\begin{cases} \tan\varphi_1 = \dfrac{y}{x} \\ \tan\varphi_2 = \dfrac{y}{x_2 - x} \end{cases} \quad (28)$$

then the operator can be positioned easily

$$\begin{cases} x = \dfrac{x_2 \tan\varphi_2}{\tan\varphi_1 + \tan\varphi_2} \\ y = \dfrac{\tan\varphi_1 \tan\varphi_2}{\tan\varphi_1 + \tan\varphi_2} \end{cases} \quad (29)$$

besides, we know from the (29), the elevation θ_1 and θ_2 are not necessary, then (27) can be simplified as

$$\begin{cases} \varphi = \arctan\Big(\dfrac{\sin\varphi}{\cos\varphi}\Big), & \text{if } \varphi \in (0, \pi/2) \\ \varphi = \pi + \arctan\Big(\dfrac{\sin\varphi}{\cos\varphi}\Big), & \text{if } \varphi \in (\pi/2, \pi) \\ \varphi = \pi + \arctan\Big(\dfrac{\sin\varphi}{\cos\varphi}\Big), & \text{if } \varphi \in (\pi, \dfrac{3}{2}\pi) \\ \varphi = 2\pi + \arctan\Big(\dfrac{\sin\varphi}{\cos\varphi}\Big), & \text{if } \varphi \in (\dfrac{3}{2}\pi, 2\pi) \end{cases} \quad (30)$$

The proposed algorithm is based on the SVR and two-point positioning model, so it can be called SVR-T, then according to the derivation above, we can summarize the steps of the algorithm above:

(1) Generate training samples. Solve and decompose the covariance of received data, then extract the signal subspace $\boldsymbol{x} = \boldsymbol{U}_S$ as the input feature, define $\boldsymbol{y} = (\cos\varphi, \sin\varphi)$ as output feature, then the training samples $\Theta = \{(x_i, y_i) | i = 1, 2, \cdots N_1\}$ is acquired, where N_1 is the number of training samples.

(2) Training the SVR model. Define $\boldsymbol{x} = \boldsymbol{U}_S$, $\boldsymbol{y} = (\cos\varphi, \sin\varphi)$ as input and output parameters respectively to training the SVR model, where a_i, q_g, σ, and b can be determined by some optimization algorithm.

(3) Generate test sample. Change the DOA, then extract the signal subspace $\boldsymbol{U}_S$, thus, input feature $\boldsymbol{x} = \boldsymbol{U}_S$ is obtained.

(4) Estimate DOA. Take the test sample $\boldsymbol{x} = \boldsymbol{U}_S$ into the trained SVR, we will get the sine and cosine of DOA, then the estimation can be evaluated with (29).

(5) Modified the SVR parameters according to the estimation result properly.

In fact, we can also locate the operator through single-point positioning model, as it is shown in Fig.5, only one RA1 with several array sensors and an infrared range finding sensor is used, then the operator position can be detected by the height z_1 and the measured DOA φ_1, θ_1, that is

$$\begin{cases} x = z_1 \tan\theta_1 \cot\varphi_1 \\ y = z_1 \tan\theta_1 \tan\varphi_1 \end{cases} \quad (31)$$

thus, RA2 is omitted, but an additional infrared range finder is needed, as it utilizes single-point positioning model, we can called it SVR-S. In practical applications, we need to draw up the specific plan in accordance with the actual situation.

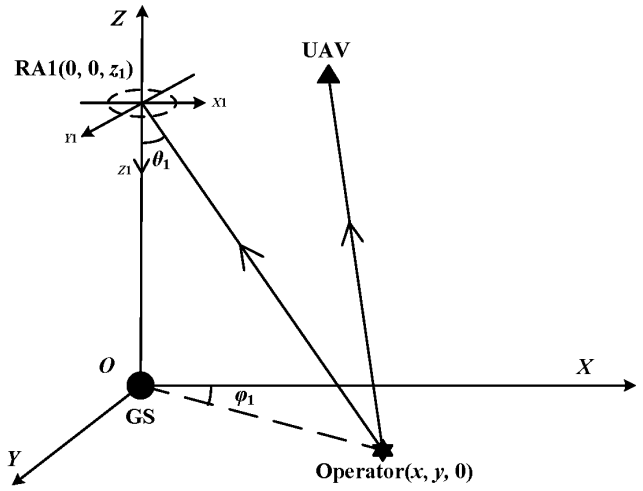

FIGURE 5. Single-point positioning model.

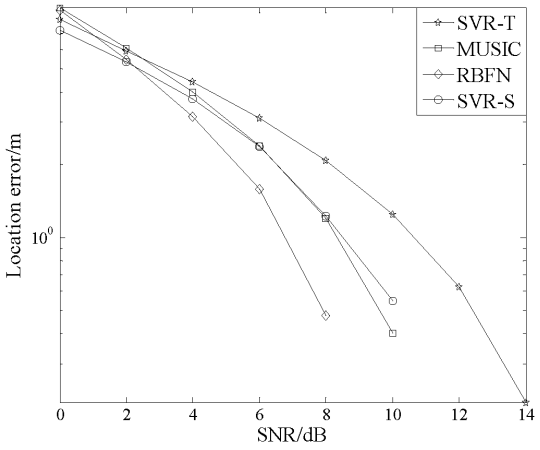

FIGURE 6. Location errors versus SNR.

V. SIMULATION

Next, we will test the performance of the proposed algorithms, the arrays on the two RAs are both composed of ten sensors, assume that the distance between two RAs is $z_1 = z_2 = x_2 = 100$m, azimuth and elevation separately range in $(0, 360°)$ and $(0, 90°)$, and the interval of training samples are both $0.1°$, the frequencies of the operator signals are all 2.4GHz, the array radius $r = 0.06$m. For test samples, $N_2 = 200$ random locations in $X \in [-1000\text{m}, 1000\text{m}]$ and $Y \in [-1000\text{m}, 1000\text{m}]$ plane are successively chosen, location estimation error is specified as $\varepsilon = \frac{1}{N_2} \sum_{n_2=1}^{N_2} \sqrt{(x_{n_2} - \hat{x}_{n_2})^2 + (y_{n_2} - \hat{y}_{n_2})^2}$, where (x_{n_2}, y_{n_2}) is the real location of the operator, $(\hat{x}_{n_2}, \hat{y}_{n_2})$ is its estimation. In the first four examples, there is no error in the array, we respectively employ MUSIC, radial basis function network (RBFN) [43], the proposed SVR-T and SVR-S to calculate DOA of only one operator, the corresponding searching step sizes of azimuth and elevation of MUSIC are both $0.1°$. In SVR-T and SVR-S, Gaussian and polynomial kernel functions are employed concurrently, Fig.6 presents their location errors versus SNR when sampling number T is 90.

We can see from Fig.6, all the four algorithms can locate the signals exactly at high SNR, and SVR-T, SVR-S are better at low SNR, but with the increasing of SNR, the other two algorithms improve faster.

In the second experiment, there is no error in the array, Fig.7 presents the location errors versus test sampling times when SNR is 14dB, we can see that the precisions of SVR-S and SVR-T are higher than that of MUSIC and RBFN at small samples, with the increasing of sampling number, the latter two algorithms perform better than the first two.

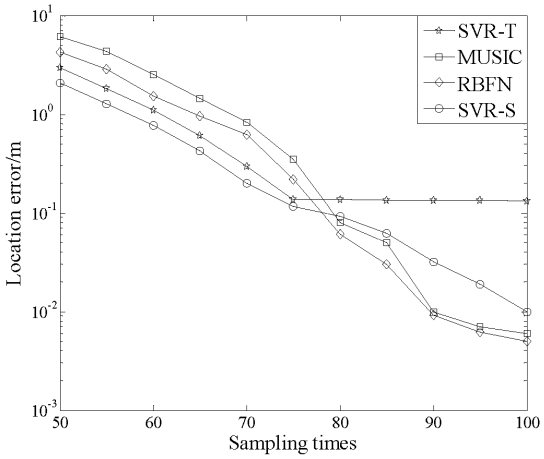

FIGURE 7. Location errors versus sampling times.

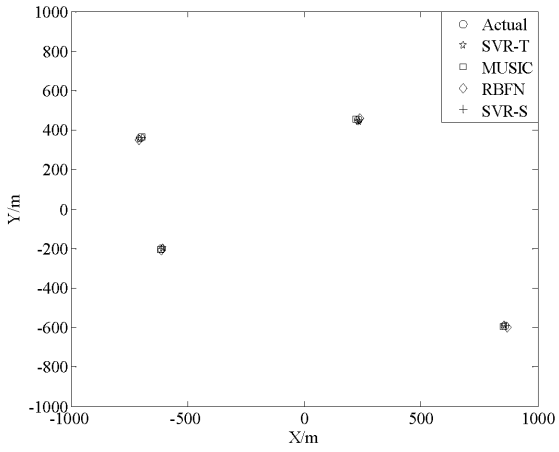

FIGURE 8. Location results of the three algorithms.

In the third experiment, let us consider the location for four signals, suppose that they comes from (230m, 450m), (−700m, 360m), (−610m, −200m), and (860m, −590m) with the same powers simultaneously, SNR is 16dB, there is no error in the array, the average of 500 trials is specified as the final result, Fig.8 gives the location result of the four algorithms, and Table 1 displays their location time.

We can observe from Fig.8, all the four algorithms can locate these signals in the four quadrants accurately, and the estimated positions of SVR-T and SVR-S are nearer than that of MUSIC and RFBN at this circumstance.

Meanwhile, we can see from Table 1, though SVR-T and SVR-S take a long time for training, their test time are shorter than the other two algorithms.

TABLE 1. Average running time.

Algorithms	Training Times	Test Time
SVR-T	2.944s	0.045s
MUSIC	0s	0.186s
RBFN	30.11s	0.052s
SVR-S	2.943s	0.045s

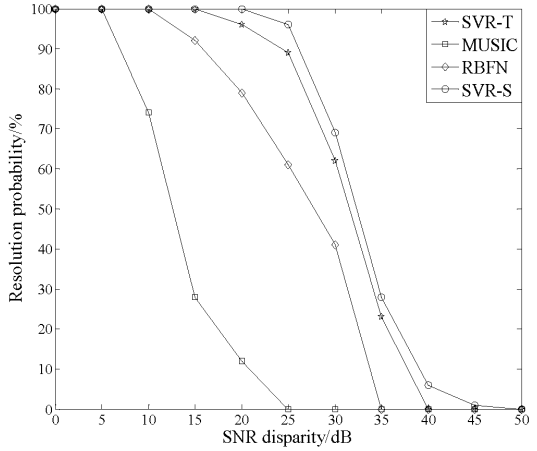

FIGURE 9. Resolution probabilities of the three algorithms.

In the fourth experiment, suppose that two operators each control a UAV, their signals impinge on the array with different SNR, and closer to each other, their DOA are separately $(\bar{\varphi}_1, \bar{\theta}_1)$ and $(\bar{\varphi}_2, \bar{\theta}_2)$, while $(\bar{\varphi}'_1, \bar{\theta}'_1)$ and $(\bar{\varphi}'_2, \bar{\theta}'_2)$ are the corresponding estimations, if $|\bar{\varphi}_k - \bar{\varphi}'_k| < \frac{|\bar{\varphi}_1 - \bar{\varphi}_2|}{2}$, $k = 1, 2$ and $|\bar{\theta}_k - \bar{\theta}'_k| < \frac{|\bar{\theta}_1 - \bar{\theta}_2|}{2}$, $k = 1, 2$, we will think that they can been distinguished. Here, we define $\bar{\varphi}_1 = 60°$, $\bar{\theta}_1 = 15°$, $\bar{\varphi}_2 = 65°$, $\bar{\theta}_2 = 20°$, there is no error in the array, SNR of the first signal is 10dB, that of the second signal is gradually increasing from 10dB, Fig.9 shows the resolution probability versus their SNR disparity.

We know from Fig.9, when the SNR disparity is lower, all the four algorithms can resolve the two signals. As SNR of the second signal increases, all of them gradually lose their effectiveness, where the proposed SVR-S has the best adaptability to SNR disparity, and SVR-T has little difference with it. So we know even though SNR of the two sources are not the same, provided the disparity is not too large, the proposed algorithms remain effective.

In the experiments below, we will consider the positioning performance with gain-phase inconsistency array, for SVR-T algorithm, the inconsistency between two RAs are the same, and they are generated according to the following equation

$$\rho_m = 1 + \zeta_m, \phi_m = 60° \times \varsigma_m \ \ (m = 1, \cdots M) \qquad (32)$$

where ζ_m, ς_m are independent and both randomly distribute in $[-0.4, 0.4]$.

Suppose there is one signal coming from (100m,100m), Fig.10 demonstrates the location errors of the four algorithms

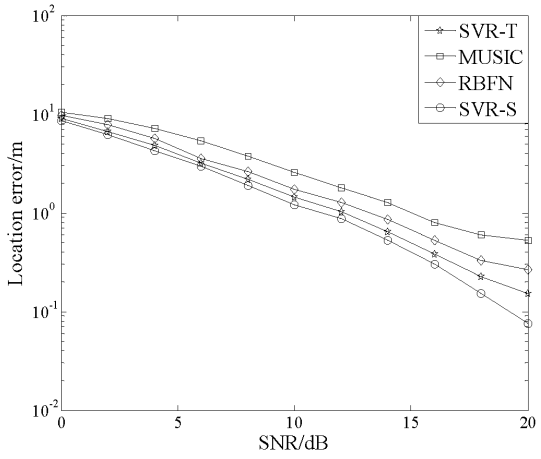

FIGURE 10. Location errors based on the array with gain inconsistency.

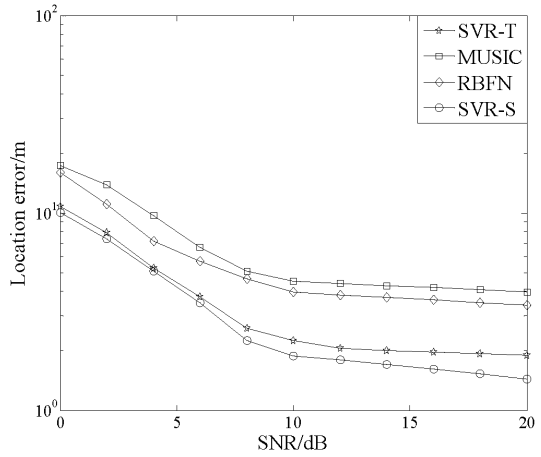

FIGURE 11. Location errors based on the array with phase inconsistency.

versus SNR when only gain inconsistency exists in the array sensors, Fig.11 gives the result based on the array sensor with phase inconsistency, we observe that the estimation precisions of all the algorithms decline comparing with that under ideal array. Comparatively speaking, the effect of phase inconsistency is much more serious than that of gain inconsistency.

Then let us talk about the situation when both inconsistency exist simultaneously, we still suppose that the signal impinges from (100m,100m), Fig.12 displays the location errors of the four algorithms versus SNR, we find that their location performances are all worse than that when the two inconsistencies independently exist, but the proposed SVR-S and SVR-T are still more effective than the other two algorithms.

Finally, we test the performance of single kernel and multiple kernel learning. In this section, we take SVR-S for the trial, Gaussian, polynomial, and the combination of them are separately exploited, Fig.13 illustrates the selection results of them. We know from Fig.13, the MKL has a better capability of approximation than the single learning, and it is properer to deal with the gain-phase error calibration in the array sensors.

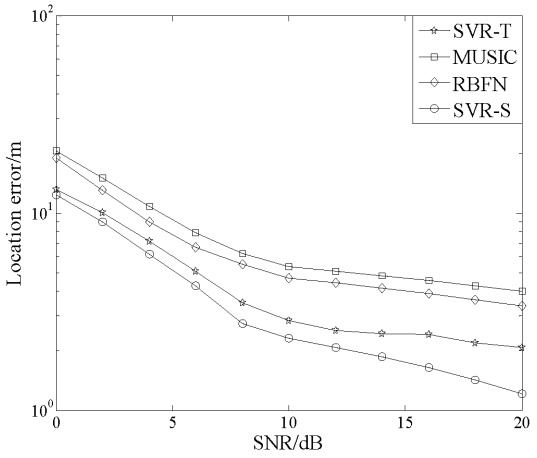

FIGURE 12. Location errors based on the array with gain-phase inconsistency.

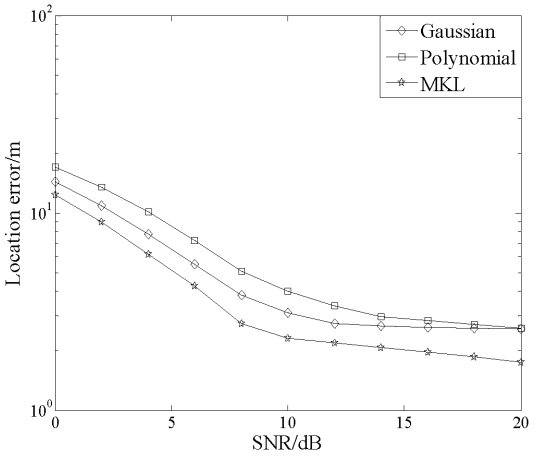

FIGURE 13. Location errors based on the different kernels.

VI. CONCLUSION

In this paper, an algorithm for detecting the location of UAV operator is proposed, based on SVR, we employ RA to estimate the DOA of the UAV operators, then locate them according to the geometrical relationship. Comparing with some traditional algorithms, it is especially applicable to the conditions of low SNR and small samples. Moreover, due to the use of super-resolution algorithm and MKL, we can still deal with multiple operator signals under gain-phase inconsistency sensor array. However, it is just in the theoretical research stage, in the future, we will use hardware to implement the algorithm, so as to explore its practical applications.

ACKNOWLEDGMENT

The author would like to thank Prof. Q. Ding, and all the editors and reviewers of this paper.

REFERENCES

[1] C. Joo and J. Choi, "Low-delay broadband satellite communications with high-altitude unmanned aerial vehicles," *J. Commun. Netw.*, vol. 20, no. 1, pp. 102–108, Feb. 2018.

[2] K. Saito, Q. Fan, N. Keerativoranan, and J.-I. Takada, "Vertical and horizontal building entry loss measurement in 4.9 GHz band by unmanned aerial vehicle," *IEEE Wireless Commun. Lett.*, vol. 8, no. 2, pp. 444–447, Apr. 2019.

[3] E. C. Tetila, B. B. Machado, N. A. de Souza Belete, D. A. Guimarães, and H. Pistori, "Identification of soybean foliar diseases using unmanned aerial vehicle images," *IEEE Geosci. Remote Sens. Lett.*, vol. 14, no. 12, pp. 2190–2194, Dec. 2017.

[4] S. Jung, H. Cho, D. Kim, K. Kim, J. Han, and H. Myung, "Development of algal Bloom removal system using unmanned aerial vehicle and surface vehicle," *IEEE Access*, vol. 5, pp. 22166–22176, 2017.

[5] A. Alexandridis and A. Mouchtaris, "Multiple sound source location estimation in wireless acoustic sensor networks using DOA estimates: The data-association problem," *IEEE/ACM Trans. Audio, Speech, Language Process.*, vol. 26, no. 2, pp. 342–356, Feb. 2018.

[6] J. Werner, J. Wang, A. Hakkarainen, D. Cabric, and M. Valkama, "Performance and Cramér–Rao bounds for DoA/RSS estimation and transmitter localization using sectorized antennas," *IEEE Trans. Veh. Technol.*, vol. 65, no. 5, pp. 3255–3270, May 2016.

[7] Z. Wei, Y. Zhao, X. Liu, and Z. Feng, "DoA-LF: A location fingerprint positioning algorithm with millimeter-wave," *IEEE Access*, vol. 5, pp. 22678–22688, 2017.

[8] H. Wang, L. Wan, M. Dong, K. Ota, and X. Wang, "Assistant vehicle localization based on three collaborative base stations via SBL-based robust DOA estimation," *IEEE Internet Things J.*, vol. 6, no. 3, pp. 5766–5777, Jun. 2019.

[9] C.-H. Park and J.-H. Chang, "TOA source localization and DOA estimation algorithms using prior distribution for calibrated source," *Digit. Signal Process.*, vol. 71, pp. 61–68, Dec. 2017.

[10] M. R. Gholami, S. Gezici, and E. G. Ström, "TW-TOA based positioning in the presence of clock imperfections," *Digit. Signal Process.*, vol. 59, pp. 19–30, Dec. 2016.

[11] Y. Liu, F. Guo, L. Yang, and W. Jiang, "Source localization using a moving receiver and noisy TOA measurements," *Signal Process.*, vol. 119, pp. 185–189, Feb. 2016.

[12] E. Kazikli and S. Gezici, "Hybrid TDOA/RSS based localization for visible light systems," *Digit. Signal Process.*, vol. 86, pp. 19–28, Mar. 2019.

[13] D. Wang, J. Yin, T. Tang, X. Chen, and Z. Wu, "Quadratic constrained weighted least-squares method for TDOA source localization in the presence of clock synchronization bias: Analysis and solution," *Digit. Signal Process.*, vol. 82, pp. 237–257, Nov. 2018.

[14] Y. Sun, K. C. Ho, and Q. Wan, "Solution and analysis of TDOA localization of a near or distant source in closed form," *IEEE Trans. Signal Process.*, vol. 67, no. 2, pp. 320–335, Jan. 2019.

[15] S. Tomic, M. Beko, and M. Tuba, "A linear estimator for network localization using integrated RSS and AOA measurements," *IEEE Signal Process. Lett.*, vol. 26, no. 3, pp. 405–409, Mar. 2019.

[16] N. H. Nguyen and K. Doğançay, "Instrumental variable based Kalman filter algorithm for three-dimensional AOA target tracking," *IEEE Signal Process. Lett.*, vol. 25, no. 10, pp. 1605–1609, Oct. 2018.

[17] N. Garcia, H. Wymeersch, and D. T. M. Slock, "Optimal precoders for tracking the AoD and AoA of a mmWave path," *IEEE Trans. Signal Process.*, vol. 66, no. 21, pp. 5718–5729, Nov. 2018.

[18] P. Abouzar, D. G. Michelson, and M. Hamdi, "RSSI-based distributed self-localization for wireless sensor networks used in precision agriculture," *IEEE Trans. Wireless Commun.*, vol. 15, no. 10, pp. 6638–6650, Oct. 2016.

[19] A. E. Lagias, T. D. Lagkas, and J. Zhang, "New RSSI-based tracking for following mobile targets using the law of cosines," *IEEE Wireless Commun. Lett.*, vol. 7, no. 3, pp. 392–395, Jun. 2018.

[20] J. Luomala and I. Hakala, "Analysis and evaluation of adaptive RSSI-based ranging in outdoor wireless sensor networks," *Ad Hoc Netw.*, vol. 87, pp. 100–112, May 2019.

[21] Z. Na, Y. Wang, X. Li, J. Xia, X. Liu, M. Xiong, and W. Lu, "Subcarrier allocation based simultaneous wireless information and power transfer algorithm in 5G cooperative OFDM communication systems," *Phys. Commun.*, vol. 29, pp. 164–170, Aug. 2018.

[22] Z. Na, J. Lv, M. Zhang, B. Peng, M. Xiong, and M. Guan, "GFDM based wireless powered communication for cooperative relay system," *IEEE Access*, vol. 7, pp. 50971–50979, 2019.

[23] M. Shalaby, M. Shokair, and N. W. Messiha, "Performance enhancement of TOA localized wireless sensor networks," *Wireless Pers. Commun.*, vol. 95, no. 4, pp. 4667–4679, Aug. 2017.

[24] S. Tomic, M. Beko, and R. Dinis, "A robust bisection-based estimator for TOA-based target localization in NLOS environments," *IEEE Commun. Lett.*, vol. 21, no. 11, pp. 2488–2491, Nov. 2017.
[25] J. M. Pak, C. K. Ahn, P. Shi, Y. S. Shmaliy, and M. T. Lim, "Distributed hybrid particle/FIR filtering for mitigating NLOS effects in TOA-based localization using wireless sensor networks," *IEEE Trans. Ind. Electron.*, vol. 64, no. 6, pp. 5182–5191, Jun. 2017.
[26] Y. Liu, F. Guo, L. Yang, and W. Jiang, "An improved algebraic solution for TDOA localization with sensor position errors," *IEEE Commun. Lett.*, vol. 19, no. 12, pp. 2218–2221, Dec. 2015.
[27] H.-J. Shao, X.-P. Zhang, and Z. Wang, "Efficient closed-form algorithms for AOA based self-localization of sensor nodes using auxiliary variables," *IEEE Trans. Signal Process.*, vol. 62, no. 10, pp. 2580–2594, May 2014.
[28] L. Gui, M. Yang, P. Fang, and S. Yang, "RSS-based indoor localisation using MDCF," *IET Wireless Sensor Syst.*, vol. 7, no. 4, pp. 98–104, Aug. 2017.
[29] M. Angjelichinoski, D. Denkovski, V. Atanasovski, and L. Gavrilovska, "Cramér–Rao lower bounds of RSS-based localization with anchor position uncertainty," *IEEE Trans. Inf. Theory*, vol. 61, no. 5, pp. 2807–2834, May 2015.
[30] F. Gustafsson and F. Gunnarsson, "Mobile positioning using wireless networks: Possibilities and fundamental limitations based on available wireless network measurements," *IEEE Signal Process. Mag.*, vol. 22, no. 4, pp. 41–53, Jul. 2005.
[31] M. Singh and P. M. Khilar, "An analytical geometric range free localization scheme based on mobile beacon points in wireless sensor network," *Wireless Netw.*, vol. 22, no. 8, pp. 2537–2550, Nov. 2016.
[32] R. O. Schmidt, "Multiple emitter location and signal parameter estimation," *IEEE Trans. Antennas Propag.*, vol. 34, no. 3, pp. 276–280, Mar. 1986.
[33] R. Roy, A. Paulraj, and T. Kailath, "ESPRIT—A subspace rotation approach to estimation of parameters of cisoids in noise," *IEEE Trans. Acoust., Speech, Signal Process.*, vol. 34, no. 5, pp. 1340–1342, Oct. 1986.
[34] P. Stoica and A. Nehorai, "MUSIC, maximum likelihood and Cramér–Rao bound," in *Proc. Int. Conf. Acoust., Speech, Signal Process.*, New York, NY, USA, Apr. 1988, pp. 2296–2299.
[35] A. El Gonnouni, M. Martinez-Ramon, J. L. Rojo-Alvarez, G. Camps-Valls, A. R. Figueiras-Vidal, and C. G. Christodoulou, "A support vector machine MUSIC algorithm," *IEEE Trans. Antennas Propag.*, vol. 60, no. 10, pp. 4901–4910, Oct. 2012.
[36] M. Dehghanpour, V. T. T. Vakili, and A. Farrokhi, "DOA estimation using multiple kernel learning SVM considering mutual coupling," in *Proc. 4th Int. Conf. Intell. Netw. Collaborative Syst.*, Bucharest, Romania, Sep. 2012, pp. 55–61.
[37] Y. Gao, D. Hu, Y. Chen, and Y. Ma, "Gridless 1-b DOA estimation exploiting SVM approach," *IEEE Commun. Lett.*, vol. 21, no. 10, pp. 2210–2213, Oct. 2017.
[38] D. Wang, Y. Zou, and W. Wang, "Learning soft mask with DNN and DNN-SVM for multi-speaker DOA estimation using an acoustic vector sensor," *J. Franklin Inst.*, vol. 355, no. 4, pp. 1692–1709, Mar. 2018.
[39] J. Rissanen, "Modeling by shortest data description," *Automatica*, vol. 14, no. 5, pp. 465–471, Sep. 1978.
[40] H. Akaike, "A new look at the statistical model identification," *IEEE Trans. Autom. Control*, vol. 19, no. 6, pp. 716–723, Dec. 1974.
[41] V. N. Vapnik, *The Nature of Statistical Learning Theory*. Berlin, Germany: Springer, 1995, pp. 119–166.
[42] V. N. Vapnik, *Statistical Learning Theory*. New York, NY, USA: Wiley, 1998, pp. 19–68.
[43] M. Wang, S. Yang, S. Wu, and F. Luo, "A RBFNN approach for DOA estimation of ultra wideband antenna array," *Neurocomputing*, vol. 71, nos. 4–6, pp. 631–640, Jan. 2008.

JIAQI ZHEN (M'18) was born in Harbin, Heilongjiang, China, in 1981. He received the master's and Ph.D. degrees from the College of Information and Communication Engineering, Harbin Engineering University, Harbin, in 2007 and 2011, respectively.

From 2011 to 2015, he was a Lecturer in the major of communication engineering with Heilongjiang University, Harbin. Since 2015, he has been an Associate Professor in the major of the Internet of Things engineering with Heilongjiang University, the Director of the Institute of Instrumentation. He has published an academic monograph, two textbooks, more than 30 articles, and 15 inventive patents. His research interests include spatial spectrum estimation, indoor positioning, array signal parameter estimation, and embedded system design. He received the Best Paper at the Second EAI International Conference on Advanced Hybrid Information Processing, in 2018.